Published in final edited form as:
Acad Radiol. 2006 November ; 13(11): 1344–1354.

Morphologic Blooming in Breast MRI as a Characterization of Margin for Discriminating Benign from Malignant Lesions

Alan Penn, Ph.D.,
Penn Diagnostics, Address: 14 Clemson Ct., Rockville, Md. 20850, Phone: (301) 279-5958, Fax: (301) 838-0288

Scott Thompson, Ph.D.,
Penn Diagnostics

Rachel Brem, M.D.,
The George Washington University Medical Center

Constance Lehman, M.D., Ph.D.,
University of Washington Medical Center

Paul Weatherall, M.D.,
University of Texas Southwestern Medical Center

Mitchell Schnall, M.D., Ph.D.,
Hospital of the University of Pennsylvania

Gillian Newstead, M.D.,
University of Chicago

Emily Conant, M.D.,
Hospital of the University of Pennsylvania

Susan Ascher, M.D.,
Georgetown University Hospital

Elizabeth Morris, M.D., and
Memorial Sloan-Kettering Cancer Center

Etta Pisano, M.D.
University of North Carolina School of Medicine

Abstract

OBJECTIVES— Develop a fully automated, objective method for evaluating morphology on breast MR and evaluate effectiveness of the new morphological method for detecting breast cancers.

SUBJECTS AND METHODS— We present a new automated method (Morphological Blooming) for identifying and classifying breast lesions on MR which measures margin sharpness, a characteristic related to blooming, defined as rapid enhancement, with a border that is initially sharp but becomes unsharp after seven minutes. Independent training sets (98 biopsy-proven lesions) and testing sets (179 breasts, 127 patients, acquired at 5 institutions) were used. Morphological Blooming was evaluated as a stand-alone feature and as an adjunct to kinetics using FROC (free-response ROC)

Correspondence to: Alan Penn, apenn@ONCAD.com.

and sensitivity analysis. Dependence of false positive (FP) rates on acquisition times and pathologies of contralateral breasts were evaluated.

RESULTS— Sensitivity of Morphological Blooming was 80% with 2.46 false positives (FP) per non-cancerous breast: FPs did not vary significantly by acquisition times. FPs varied significantly by pathologies of contralateral breasts (cancerous contralateral: 4.29 FP/breast; non-cancerous contralateral: 0.48 FP/breast; $p<.0001$). Evaluation of 45 cancers showed suspicious morphologies on 10/15 (67%) cancers with benign-like kinetics and suspicious kinetics on 5/10 (50%) cancers with benign-like morphologies.

CONCLUSION— We present a new, fully automated method of identifying and classifying margin sharpness of breast lesions on MR that can be used to direct radiologists' attention to lesions with suspicious morphologies. Morphological Blooming may have important utility for assisting radiologists in identifying cancers with benign-like kinetics and discriminating normal tissues that exhibit cancer-like enhancement curves and for improving the performance of CAD systems.

Studies have demonstrated the effectiveness of breast MRI for improving breast cancer detection and diagnosis [1,2,3,4,5,6,7]. Breast MRI presents the breast imager with two challenges: low specificity, which can result in a clinically unacceptable number of false positives [8,9], and a large number of images that must be interpreted. Recent screening studies in Netherlands, Canada, and United Kingdom have reported breast cancer sensitivities using MRI ranging from 71%–77% [3]. A follow-up of the MARIBS study in the United Kingdom found that independent double-reading of breast MRI improved sensitivity by 7% [10]. To address these challenges, breast MRI computer-aided-detection (CAD) systems have been developed to help radiologists more easily sort through images and focus on suspicious areas of enhancement to improve efficiencies in interpreting breast MRI.

Interpretive features that are used to discriminate malignant from benign lesions on breast MRI fall into two general categories: kinetics, based on the rate and degree an enhancing agent washes into and out of a region-of-interest, and morphology, based on the shape and texture of the enhancement pattern [11]. Some cancers, particularly invasive lobular [7,12], DCIS [12,13,14], and scirrhous ductal invasive cancers [7], often fail to exhibit cancer-like kinetics. Moreover, some benign conditions, such as fibroadenomas and hyperplasia produce dynamic patterns similar to malignancies [15]. The American College of Radiology recommends that radiologists evaluate both kinetic and morphologic characteristics [16].

Commercialized breast MRI CAD systems have relied primarily on kinetic analysis for detecting suspicious regions [17]. While there has been research in computer analysis of morphology [18,19,20], clinical assessment still relies on reader interpretation to evaluate morphology [4,21]. Studies on morphological measures for breast MRI have evaluated shape, texture, orientation, intensity, gradients, and other factors that model tissues in the breast [18, 22,23,24]. None of the previously reported morphological measures has been shown to be sufficiently robust, effective, and computationally efficient to be included in a commercialized breast MRI CAD system. There is a clinical need for including morphological analysis into CAD systems to assist radiologists in the detection of cancers and differentiation of benign from malignant lesions [17].

Another serious and challenging problem is observer variability in evaluation of lesion morphology. Mussurakis, et al. reported kappa statistics between pairs of radiologists who interpreted contours (defined as: (a) well-defined, (b) partially well-defined, (c) irregular, spiculated, or (d) irregular, nonspecific) on T1 weighted post-contrast breast MRI images as 0.34, 0.23, 0.34 [25]. Kinkel, et al. found an interobserver variability for margins (dichotomous selection of: (a) smooth or unable to assess, and (b) irregular or spiculated) of 0.29 [26]. Kappa statistics in the range 0.21–0.40 are considered to be "fair" agreement [27]. These results

indicate a need to develop methods to decrease the variability of breast MRI interpretation. Fully automated computer-generated features have no user variability and offer a means for addressing this issue.

This paper presents analysis of a new objective method of identifying and classifying MRI breast lesions on the basis of margin sharpness that is substantially different from the morphological methods that have been reported previously. The method is fully automated and can be used to direct the radiologist's attention to lesions that have suspicious morphologies. The new method may be particularly helpful for identifying cancers that lack suspicious kinetic patterns. Prior studies have used subjective interpretations of margin characterization and blooming, and such interpretations are dependent upon the experience of the radiologist. [28, 29]. The new feature presented here is generated by the computer without user input, which increases objectivity and reproducibility, and simplifies MR analysis.

Subjects and Methods

Data

Independent data sets were used for the training and testing of the Morphological Blooming feature. All images were T1-weighted, fat suppressed, and acquired on 1.5T MRI systems with dedicated breast coils. For cases containing biopsied lesions, a site principal investigator (P.I.) at the acquiring institution identified the location of the lesions that were biopsied and provided the pathologic diagnoses. At each institution, IRB approval or exemption from review was obtained. Data for training cases consisted of binary files containing intensity levels of pre- and post-contrast T1 images and a summary statement of the protocol used to acquire the images. Data for testing cases consisted of DICOM-compliant files that contained both image and protocol data. For the testing cases, times of acquisition were estimated from the DICOM header by subtracting the recorded time of the last pre-contrast image from the recorded time of the post-contrast image. The following definitions are used: "normal" is a breast where no lesion was found; "benign" is a breast with a biopsy-proven benign lesion and no indication of cancer; "non-cancerous" is either normal or benign; "non-cancerous, contralateral to cancer" is normal or benign with known cancer in the other breast; "non-cancerous, contralateral to non-cancerous" is normal or benign with no cancer in the other breast; "non-cancerous, contralateral to unknown" is normal or benign with no information about the other breast. A breast is called "cancer" if it contains a biopsy-proven cancerous lesion.

Analysis of false positives (FP) was based exclusively on benigns and normals. Although FPs can occur in breasts with known cancers, they are ignored in the FP analysis since we had insufficient biopsy information to determine the location and extent of cancers throughout the breast.

Data set used for training Morphological Blooming feature

Training of the feature was performed using two-dimensional images of biopsy-proven focal masses. The training data set consisted of 98 cases (43 Benign; 55 Cancer) acquired using a three-dimensional fat-suppressed, radiofrequency, spoiled gradient-echo sequence on a 1.5T system with a Signa console (GE Medical Systems). The first post-contrast images were obtained during the first 90 seconds after the delivery of a 20-mL bolus of a gadolinium-based contrast agent, gadopentetate dimeglumine (Magnevist: Berlex, Wayne, NJ). The scan was initiated after gadolinium injection but prior to a 20ml saline flush. Subsequent images of the breast were taken immediately following the first post-contrast image. The resulting sagittal images consist of 512x512 pixels and were obtained from an acquisition matrix of 512x256x32. Field of view ranged from 16 to 22 cm, and slice thicknesses ranged from 1.5 to 4.0 mm, depending on the size of the breast. Flip angle was ≤45.

Data set used for testing Morphological Blooming feature

Only images of non-cancerous breasts (benigns and normals) and breasts with biopsy-proven cancers were used. Since a true positive finding was recorded only when the location of a biopsy-proven cancer was marked, breasts that were assessed as being cancer but where biopsy results were not available were excluded from the study. Breasts in the testing set included cancers (71), normals (53), and benigns (55) from 127 patients. Of the cancers, 37 were infiltrating ductal, 6 infiltrating lobular, 4 infiltrating mixed ductal and lobular, 17 DCIS, 1 medullary, 6 unspecified. Of the normals, 28 were contralateral to cancer, 8 contralateral to normal, 17 contralateral to benign. Of the benigns, 17 were contralateral to normal, 10 contralateral to benign, and 28 contralateral to unknown. 35 non-cancerous breasts had follow-ups of at least 12 months and 4 had follow-ups 6–12 months; the remaining 69 non-cancerous breasts were assessed on the basis of radiologists' interpretations of images taken at the time of, or within 6 months of, the original MR study. Four patients had multiple biopsy-proven malignant lesions (three patients with two malignant lesions in one breast and none in the other breast; one patient with two malignant lesions in one breast and one malignant lesion in the other breast). The average age of patients was 48.4 years, with standard deviation 9.4 years. Institutional protocols and data are summarized in Table 1.

Images in the testing set were obtained from five institutions using a variety of clinical and research protocols which differed from the fixed protocol used for the training set. Protocol values listed in Table 1 for time delay after contrast, echo times, flip angles, slice thicknesses, and field-of-view (FOV) were obtained from DICOM headers for cases used in the study. For institutions 3, 4 and 5, long time delays between pre-contrast image and post-contrast image shown in Table 1 were due to intervening imaging of the contralateral breast after the contrast injection and before imaging of the breast used in the study. For institution 2, long delays shown in Table 1 were due to use of the third post-contrast image in the analysis, as recommended by the site Principal Investigator, to account for slow uptake of the contrast agent resulting from the lack of a saline push after injection.

Feature Overview

The lesion morphology characterization presented here is an assessment of the unsharpness of borders using the pre-contrast and a single post-contrast T1 image. The feature is related to blooming, a kinetic feature based on the physiological phenomenon of leakage from the core of the lesion to surrounding tissue due to vascularization of the lesion [29,30]. Since malignant lesions generally have greater vascularization than benign lesions, there is a greater kinetic blooming effect. Fischer, et al showed that malignant breast lesions exhibit greater kinetic blooming than benign lesions when evaluated over a seven minute time period [29].

Definition of Two-Dimensional Morphological Blooming Feature

All images were resized to 256x256 for processing. A feature value (**MB-2D**) based on the magnitude of blooming was computed independently on each two-dimensional slice for each cluster of enhancing pixels on the subtraction image using the following algorithm: (1) For each enhancing region, a high-intensity threshold was determined to be the highest intensity level that generated a cluster on the binary thresholded image exceeding 25 mm^2 (the initial cluster); (2) A nested sequence of clusters was generated from the initial cluster by successively lowering the intensity level used for binary thresholding. The process was terminated when the threshold reached the level of background tissue and the cluster expanded to include a large portion of the breast; (3) A minimal bounding box was derived for each cluster in the nested sequence. The bounding box served as a filter that reduced the effect of noise that distinguished clusters in the nested sequence; (4) A segmented enhancement was defined to be the cluster from the nested sequence of clusters that had the highest gradient and that exceeded 50 mm^2 in size. The number of distinct bounding boxes was computed and used as the feature value

for this segmented enhancement. For all cases in which a saline push was used after bolus injection, the **MB-2D** feature was evaluated on the first post-contrast image. For cases from Institution 2 for which a saline push was not used, the third post-contrast image was used.

If the lesion exhibited blooming, there was an unsharpness of the border, resulting in a large number of distinct nested boxes (high **MB-2D**); if the lesion did not exhibit blooming, the borders were sharp and a small number of distinct nested boxes were present (low **MB-2D**). Analysis of training data suggested the following additional filters to help eliminate artifacts and vessels: (1) Enhancement of at least 75% over pre-contrast image. This parameter setting is comparable to enhancement thresholds suggested in the literature [29,31], and (2) Compactness parameter (p^2/A), where p is the perimeter and A the area of the lesion, [32] must be less than or equal to 124, a value heuristically determined from the image data.

Definition of Three-Dimensional Morphological Blooming Feature

The **MB-3D** feature was formed by stacking overlapping adjacent two-dimensional enhancing regions. The stacking operation resulted in a three-dimensional enhancement that was assigned a feature values as follows: (1) For each slice in the three-dimensional enhancement, a smoothed **MB-2D** value was derived by weighting the **MB-2D** within the given slice with a factor of .5 and weighting the **MB-2D** values for enhancements in the adjacent slices with a factor of .25; (2) the maximum smoothed **MB-2D** value over the set of slices in the three-dimensional enhancement was used as the **MB-3D** feature value.

Evaluation Methodology

Performance of the Morphological Blooming feature as a sole discriminator of benign from malignant conditions was evaluated using FROC (free-response ROC) analysis which evaluates the true positive fraction (sensitivity) as a function of the number of false positives (FPs) [33]. FROC evaluation is presented as an empirical plot of data obtained from the study, without the use of model-fitting or smoothing. Sensitivity values were computed using breasts, rather than patients, as the unit being scored; for the four breasts that contained two biopsied malignant lesions, a marking on either of the lesions counted as a positive finding; for the one patient that had biopsied malignant lesions in both breasts, the two breasts were analyzed and scored independently. Similarly, FP values were computed independently for the left and right breasts in those cases that were non-cancerous in both breasts.

Definition of True Positive (TP)—For each cancer, the site P.I. selected a spatial slice that cut through the biopsied lesion and drew a two-dimensional box around the lesion on the selected slice. An expert (RB) reviewed three-dimensional image sets of cancers, and, using the two-dimensional boxes as guides, constructed three-dimensional cubes around the cancers. For each cancer, the highest **MB-3D** value from the set of three-dimensional enhancements that overlapped the expert's cube by a minimum of 200 mm^3 was evaluated and used in the FROC analysis.

Definition of False Positives (FP)—A three-dimensional enhancement on a non-cancerous breast was a false positive if the **MB-3D** value for that enhancement exceeded the threshold criteria used in the FROC analysis and if a minimum of 200 mm^3 of the enhancement was on the breast side of the chest wall (ST).

Performance of the Morphological Blooming feature as an adjunct to kinetics was evaluated using reader interpretations of kinetics from a prior reader study [34,35]. Readers were asked to interpret lesion kinetics as persistent, plateau, or washout; interpretations of "persistent" were assigned a score of 0, "plateau" a score of 1, and "washout" a score of 2. Overall reader interpretation of kinetics for each case was evaluated using the median score. Benign lesions

typically show persistent signal intensity curves while cancers more often show washout [36]. Cancer cases that had median reader interpretations of 0 or .5 were used in the current study as examples of cancer cases with benign-like kinetics.

Readers involved in this study were radiologists with varied experience in interpretation of breast MRI. A total of 35 radiologists participated, of which 3 had no experience in breast MRI interpretation, 11 had interpreted between 1 and 9 cases prior to participation in the study, 12 reported interpreting between 10 and 100 cases, and 9 reported interpreting greater than 100 cases. There was 1 radiology resident, 9 fellows in breast imaging, 17 attending radiologists and 8 site principle investigators. Fields of expertise self-reported by the radiologists included Neuroradiology (1), Nuclear (2), Ultrasound (1), Muscular-Skeletal (1), Interventional (2), Abdominal (1), Body Imaging (4), General MRI (3), Mammography-Breast-Women's Imaging (24). Radiologists were allowed to identify more than one area of expertise.

Results

FROC analysis

Fig. 1 is the empirical FROC curve showing sensitivity as a function of number of false positives (FP), using classification based solely on the three-dimensional Morphological Blooming feature. The numbers 9 through 12 above the markers are the thresholds for the Morphological Blooming feature used to compute the sensitivity and FP values. As an example, sensitivity and FP values at the marker pointed to by the arrow were computed by calling enhancements "cancer" if they had blooming values greater than or equal to 10 and calling them "benign" if they had blooming values less than 10. Higher thresholds resulted in fewer enhancements being called "cancer," leading to lower sensitivities and lower FP rates.

Analysis of False Positives (FP)

Fig. 2 shows details of the distribution of FPs at threshold 10 for the 108 non-cancerous breasts. The left bar shows that 37% of the cases had no FPs, or equivalently, for 37% of the cases, all enhancements had Morphological Blooming values less than 10. The dark bar, second from left, marks the median number of FPs.

Non-cancerous breasts averaged 0.47 FPs on 43 breasts from Institution 1 and 4.44 FPs on 43 breasts from Institution 4; difference in FP rates were statistically significant ($p<.0001$). The numbers of non-cancerous breasts from other institutions were insufficient for statistical analysis. Dependences of FP rates on two characteristics of the data sets were analyzed: (1) acquisition times of first post-contrast images (Institution 1: mean 220 seconds; Institution 4: mean 374 seconds; time difference was statistically significant ($p<.0001$)), and (2) pathologies of patient populations (Institution 1: non-cancerous contralaterals (38), cancerous contralaterals (5); Institution 4: non-cancerous contralaterals (4), cancerous contralaterals (25), unknown contralaterals (14)).

Analysis of FP rate vs. acquisition time

FP rates were computed for all series of post-contrast images with means less than 600 seconds from Institutions 1 and 4 (Institution 1: first, second, third post-contrast series; Institution 4: first post-contrast series.). Results are shown in Fig. 3. There was no statistically significant difference in FP rates among the three post-contrast series from Institution 1. All 3 post-contrast series from Institution 1 had statistically significantly lower FP rates than were found on the first post-contrast series for Institution 4 ($p<.0001$).

Analysis of FP rate vs. pathologies of contralateral breasts

FP rates on non-cancerous breasts were computed independently for patients with cancerous contralateral breasts and for patients with non-cancerous contralateral breasts. Results are shown in Table 2.

Morphological Blooming and kinetic interpretation as complementary detection methods

Analysis of combined morphological and kinetic detection was performed on 45 breasts that met the following three conditions: (1) the breast contained a biopsy-proven malignant lesion; (2) multiple readers had interpreted kinetics at the lesion; (3) MR images of the full breast were available for computer analysis. Cases in this set were interpreted by an average of 13.4 radiologists (Min=5; Max=18). The last row of Table 3 shows that 10 of 15 (67%) of cancers with benign-like kinetics were identified as having suspicious margins, and 5 of 10 (50%) of cancers with benign-like margins were interpreted as having suspicious kinetics.

Examples

Cases that demonstrate the utility of Morphological Blooming as a diagnostic criterion are shown in Figures 4–5. Images show representative slices through the lesions on the first post-contrast image after injection. Figures 4A and 5A show the original MR images; Figures 4B and 5B show Morphological Blooming maps where red indicates Morphological Blooming values greater than or equal to 10 (positive findings) and yellow indicates Morphological Blooming values equal to 8–9 (near-positive findings); Figures 4C and 5C show kinetic maps, where red indicates pixels with washout and yellow indicates pixels with plateau. Colorization for Morphological Blooming is applied over the entire segmented lesion, rather than only the border, to help radiologists easily detect suspicious regions.

Discussion

We present a new objective method of identifying areas with suspicious morphology on T1 weighted MR images of the breast. This new method evaluates unsharpness of margin on the post-contrast image nearest to peak enhancement and is believed to be related to blooming, defined as change in border sharpness between 1 and 7 minutes. The hypothesis that guided our development of the new feature is that peripheral enhancement seen at seven minutes can also be seen as a low-level enhancement on an earlier image since leakage from the core of the lesion to the surrounding tissue occurs gradually over time. Since the new feature characterizes margin sharpness, which is classified as a component of morphology in the BI-RAD lexicon, we refer to the new feature as Morphological Blooming.

Morphological Blooming offers two advantages over reader assessment of blooming based on early and late post-contrast images: (1) since Morphological Blooming is objectively measured, there is no inter-observer variability. (2) Using a single post-contrast image at peak enhancement reduces the impact of patient movement.

We have found Morphological Blooming to be effective at identifying and discriminating breast cancers using a variety of different MRI protocols and systems. One important difference among the protocols used in this study is the time of acquisition of the post-contrast images. Acquisition times varied from 115 seconds to 1713 seconds, with the larger numbers corresponding to cases in which the contralateral breast was imaged after the ipsilateral breast was completely imaged. In spite of our efforts to use different protocols, there are still clinical protocols not represented in our study. For example, our primary plane of acquisition was always sagittal with fat suppression and minimal in-plane resolution of 1 mm. It is not known if use of axial or coronal planes of acquisitions, non fat-suppressed images, or lower in-plane

resolution will affect the accuracy of the Morphological Blooming feature. Further studies are needed to validate our results for these different protocols.

Much of the data was obtained from cases acquired in prior diagnostic breast MR studies and is likely not representative of cases found in a screening environment. Differences between cases used in this study and cases found in clinical screening include: 1) 55 of 108 (51%) of the study cancer-free breasts contained suspicious benign lesions. Thus the cancer-free breasts contained a disproportionate number of hard-to-diagnose lesions; 2) Prevalence of cancer in the study data was 40%, which is significantly higher than is found in a clinical screening environment. 3) Average age of patients, 48.4, was comparable to other studies of symptomatic women [10], but considerably higher than the average ages of 40–41 reported in large, multi-center screening studies [1,3].

It has been reported that breast MRI has sensitivity approaching 100% for invasive cancers and the primary need for computer support is to improve specificity. Three recent studies of breast MRI have shown that sensitivity for high-risk screening is much lower, with reported values of 71–77%. Accordingly, there may be an important role for CAD in improving sensitivity in the high-risk screening environment. Since many breast MRI CAD systems rely on kinetics to identify suspicious areas, there may be an important role for a breast MRI CAD system that also evaluates morphology. One of the more important finding of this study was that Morphological Blooming has the potential for complementing kinetics in identifying suspicious areas. We identified 15 cancers that had benign-like kinetics and found that Morphological Blooming marked 10 of these as being suspicious. Conversely, 5 of the 10 cancers that were missed using Morphological Blooming were interpreted as having suspicious kinetics. In this limited study, a combination of Morphological Blooming and kinetic interpretation achieved a sensitivity of 89%. While the set of cases in this analysis was small, it shows the promise of Morphological Blooming as an important adjunct to kinetics in identifying breast cancers. Additional research is needed in this area to both validate the results on a larger set of cases.

Each of two institutions provided images for 40% of the non-cancerous breasts used in this study. The highly significant difference in FP rates between these two institutions prompted an analysis to try to identify the source of this difference. The institution with the larger FP rate acquired much of its data in a study in which non-cancerous breasts were predominantly contralateral to, and imaged subsequent to, breasts with known malignancies. The institution with the smaller FP rate imaged patients in which both breasts were predominantly cancer-free and generated these images using an interleaved sequence in which both breasts were imaged within four minutes after injection of the contrast agent. Thus we hypothesized that two possible sources of this difference were acquisition time and patient bias. Our analysis of images from a single institution showed there was not significant relationship between acquisition time and FP rates; this result suggests that the observed difference in FP rates between these two institutions may be due, in part, to factors other than acquisition time. Since acquisition times were estimated from DICOM header data, these estimations may have introduced errors which affected our results. A second quantifiable difference between the two sets of images was overall patient pathology. This analysis led to the intriguing finding that most of the false positives were found in breasts that were contralateral to breasts with cancer. Since synchronous contralateral breast cancer occurs in up to 6% of patients [36], it is possible that the number of false positives could be related to risk. Additional research is required to understand clinical importance of this observation.

The study was originally undertaken to develop methods of distinguishing between biopsy-proven malignant lesions and biopsy-proven benign lesions. Accordingly, the study protocol only required pathologies for specific lesions. It was only after we realized the potential of

using some of the methodologies for detecting cancer that we started investigating the whole breast and required assessment of whether the breast was normal or not. For some of the cases, there was known follow-up data, leading to a verifiable assessment of non-cancerous; for other cases, however, the assessment was made strictly on the basis of image interpretations from the original MR study. The lack of standard for what constitutes a non-cancerous breast is a major deficiency of this study.

The preliminary study results presented here show that Morphological Blooming may have important utility for assisting radiologists in identifying cancers that do not exhibit cancer-like washin-washout characteristics and in discriminating normal tissues that exhibit kinetic time curves similar to malignancies.

Acknowledgements

This research was supported by grant CA85101 from the National Cancer Institute. The authors gratefully acknowledge the help of Kathryn L. Penn for her assistance in collecting and organizing data used in this study.

References

1. Kriege M, Brekelmans CTM, Boetes C, et al. Efficacy of MRI and mammography for breast-cancer screening in women with a familial or genetic predisposition. NEJM 2004;351:427–437. [PubMed: 15282350]
2. Warner E, Plewes DB, Hill KA, et al. Surveillance of BRCA1 and BRCA2 mutation carriers with magnetic resonance imaging, ultrasound, mammography, and clinical breast examination. JAMA 2004;292:1317–1325. [PubMed: 15367553]
3. Leach MO, Brown J, Dixon AK, et al. Screening with magnetic resonance imaging and mammography of a UK population at high familial risk of breast cancer: a prospective multicenter cohort study. The Lancet 2005;365:1769–1778.
4. Wiener JI, Schilling KJ, Adami C, Obuchowski NA. Assessment of suspected breast cancer by MRI: a prospective clinical trial using a combined kinetic and morphologic analysis. AJR 2005;184:878–886. [PubMed: 15728612]
5. Thibault F, Nos C, Meunier M, et al. MRI for surgical planning in patients with breast cancer who undergo preoperative chemotherapy. AJR 2004;183:1159–1168. [PubMed: 15385323]
6. Kitagawa K, Sakuma H, Ishida N, Hirano T, Ishihara A, Takeda K. Contrast-enhanced high-resolution MRI of invasive breast cancer: correlation with histopathologic subtypes. AJR 2004;183:1805–1809. [PubMed: 15547233]
7. Kuhl CK, Mielcareck P, Klaschik S, et al. Dynamic breast MR imaging: are signal intensity time course data useful for differential diagnosis of enhancing lesions? Radiology 1999;211:101–110. [PubMed: 10189459]
8. Sardanelli F, Giuseppetti GM, Panizza P, et al. Sensitivity of MRI versus mammography for detecting foci of multifocal, multicentric breast cancer in fatty and dense breasts using the whole-breast pathologic examination as a gold standard. AJR 2004;183:1149–1157. [PubMed: 15385322]
9. Bluemke DA, Gatsonis CA, Chen MH, et al. Magnetic resonance imaging of the breast prior to biopsy. JAMA 2004;292:2735–2742. [PubMed: 15585733]
10. Warren RML, Pointon L, Thompson D, et al. Reading protocol for dynamic contrast-enhanced MR images of the breast: sensitivity and specificity analysis. Radiology 2005;236:779–788. [PubMed: 16118160]
11. Orel SG, Schnall MD. MR imaging of the breast for the detection, diagnosis, and staging of breast cancer. Radiology 2001;220:13–30. [PubMed: 11425968]
12. Kinkel K, Hylton NM. Challenges to interpretation of breast MRI. JMRI 2001;13:821–829. [PubMed: 11382939]
13. Morrow M, Strom EA, Bassett LW, et al. Standard for the management of ductal carcinoma in situ of the breast (DCIS). CA 2002;52:256–276. [PubMed: 12363325]

14. Neubauer N, Mengxia L, Kuehne-Heid R, Schneider A, Kaiser WA. High grade and non-high grade ductal carcinoma in situ on dynamic MR mammography: characteristic findings for signal increase and morphological pattern of enhancement. Br J Radiol 2003;76:3–12. [PubMed: 12595319]
15. Szabo BK, Aspelin P, Kristoffersen Wiberg M, Bone B. Dynamic MR imaging of the breast. Acta Radiologica 2003;44:379–386. [PubMed: 12846687]
16. American College of Radiology. Breast MRI Imaging. 1. Reston, VA: ACR; 2003. BI-RADS®, Breast Imaging Reporting and Data System, Breast Imaging Atlas.
17. Wood C. Computer aided detection (CAD) for breast MRI. Technology in Cancer Research & Treatment 2005;4:49–53. [PubMed: 15649087]
18. Chen W, Giger ML, Lan L, Bick U. Computerized interpretation of breast MRI: investigation of enhancement variance dynamics. Med Phys 2004;31:1076–1082. [PubMed: 15191295]
19. Wang H, Zheng B, Good WF, Wang X-H. Computerized analysis of lesions in 3D MR breast images. Medical Imaging 2001: Image Processing 2001;4322:1751–1762.
20. Gilhuijs KGA, Deurloo EE, Muller SH, Peterse JL, Schultze Kool LJ. Breast MR imaging in women at increased lifetime risk of breast cancer: clinical system for computerized assessment of breast lesions — initial results. Radiology 2002;225:907–916. [PubMed: 12461278]
21. Kelcz F, Furman-Haran E, Grobgeld D, Degani H. Clinical testing of high-spatial-resolution parametric contrast-enhanced MR imaging of the breast. AJR 2002;179:1485–1492. [PubMed: 12438042]
22. Arbach, L. Doctoral Dissertation. The University of Iowa; 2005. Breast MRI: segmentation and classification.
23. Gilhuijs KGA, Giger ML, Bick U. Computerized analysis of breast lesions in three dimensions using dynamic magnetic-resonance imaging. Med Phys 1998;25:1647–1654. [PubMed: 9775369]
24. Penn AI, Bolinger L, Schnall MD, Loew MH. Discrimination of MR images of breast masses with fractal-interpolation function models. Acad Radiol 1999;6:156–163. [PubMed: 10898034]
25. Mussurakis S, Buckley DL, Coady AM, Turnbull LW, Horsman A. Observer variability in the interpretation of contrast enhanced MRI of the breast. Br J Radiol 1996;69:1009–1016. [PubMed: 8958017]
26. Kinkel K, Helbich TH, Esserman LJ, et al. Dynamic high-spatial-resolution MR imaging of suspicious breast lesions: diagnostic criteria and interobserver variability. AJR 2000;175:35–43. [PubMed: 10882243]
27. Landis JR, Koch GG. The measurement of observer agreement for categorical data. Biometrics 1977;33:159–174. [PubMed: 843571]
28. Fischer DR, Wurdinger S, Boettcher J, Malich A, Kaiser WA. Further Signs in the Evaluation of Magnetic Resonance Mammography: A retrospective Study. Invest Radiol 2005;40(7):430–435. [PubMed: 15973134]
29. Fischer DR, Baltzer P, Malich A, et al. Is the ‘blooming sign’ a promising additional tool to determine malignancy in MR mammography? Eur Radiol 2004;14:394–401. [PubMed: 14517688]
30. Malich A, Fischer DR, Wurdinger S, et al. Potential MRI interpretation model: differentiation of benign from malignant breast masses. AJR 2005;185:964–970. [PubMed: 16177416]
31. Orel SG, Schnall MD. High risk screening working group report. JMRI 1999;10:995–1005. [PubMed: 10581518]
32. Pohlman S, Powell KA, Obuchowski NA, Chilcote WA, Grudfest-Broniatowski S. Quantitative classification of breast tumors in digitized mammograms. Med Phys 1996;23(8):1337–1345. [PubMed: 8873030]
33. Chakraborty DP, Berbaum KS. Observer studies involving detection and localization: modeling, analysis and validation. Med Phys 2004;31:2313–2330. [PubMed: 15377098]
34. Penn, AI.; Thompson, S.; Pisano, ED., et al. Evaluation of prototype computer-aided diagnosis system to assist radiologists in distinguishing benign from malignant breast lesions on MR: preliminary results of multicenter study; RSNA. 2004. p. SSJ01-04.Online at http://rsna2004.rsna.org/rsna2004/V2004/conference/event_display.cfm?em_id=4406806
35. Penn AI, Thompson SF, Brem RF, et al. Impact of CAD on radiologist’s discrimination of benign from malignant breast lesions on MR. ISMRM Thirteenth Scientific Meeting and Exhibition 2005:371.

36. Kuhl CK, Schild HH. Dynamic image interpretation of MRI of the breast. J Magn Reson Imaging 2000;12:976–974.

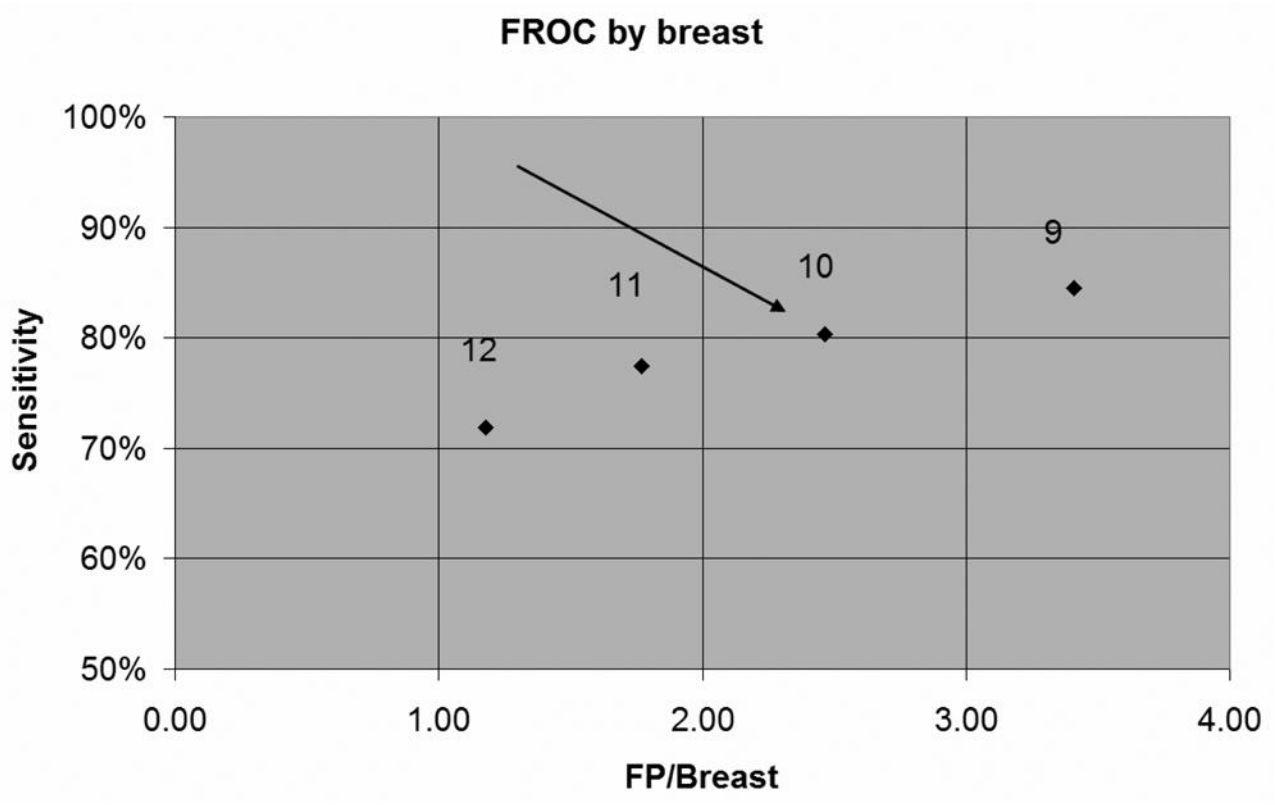

Fig 1.
FROC curve for Morphological Blooming Feature. Arrow shows operating point corresponding to threshold 10, with sensitivity=80% and 2.46 FP/Breast.

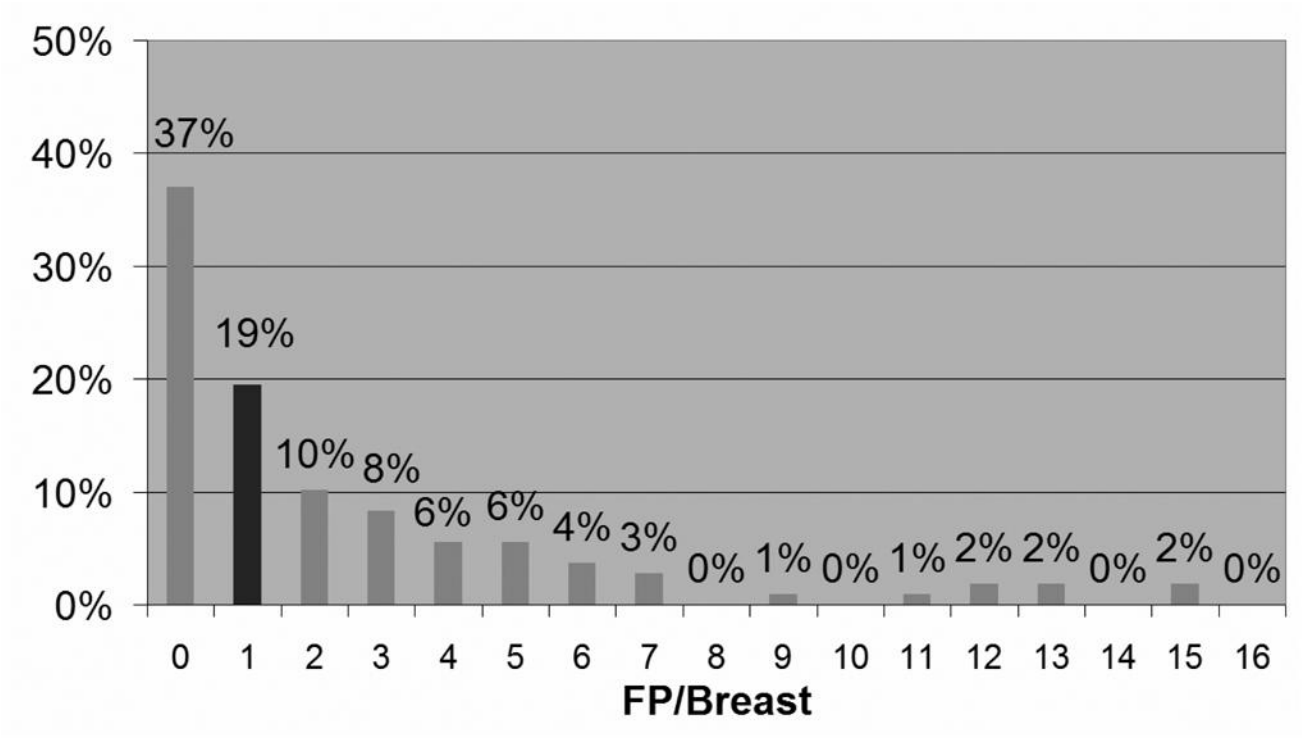

Fig 2.
Distribution of FP levels at threshold 10. Dark bar is at median number of FPs.

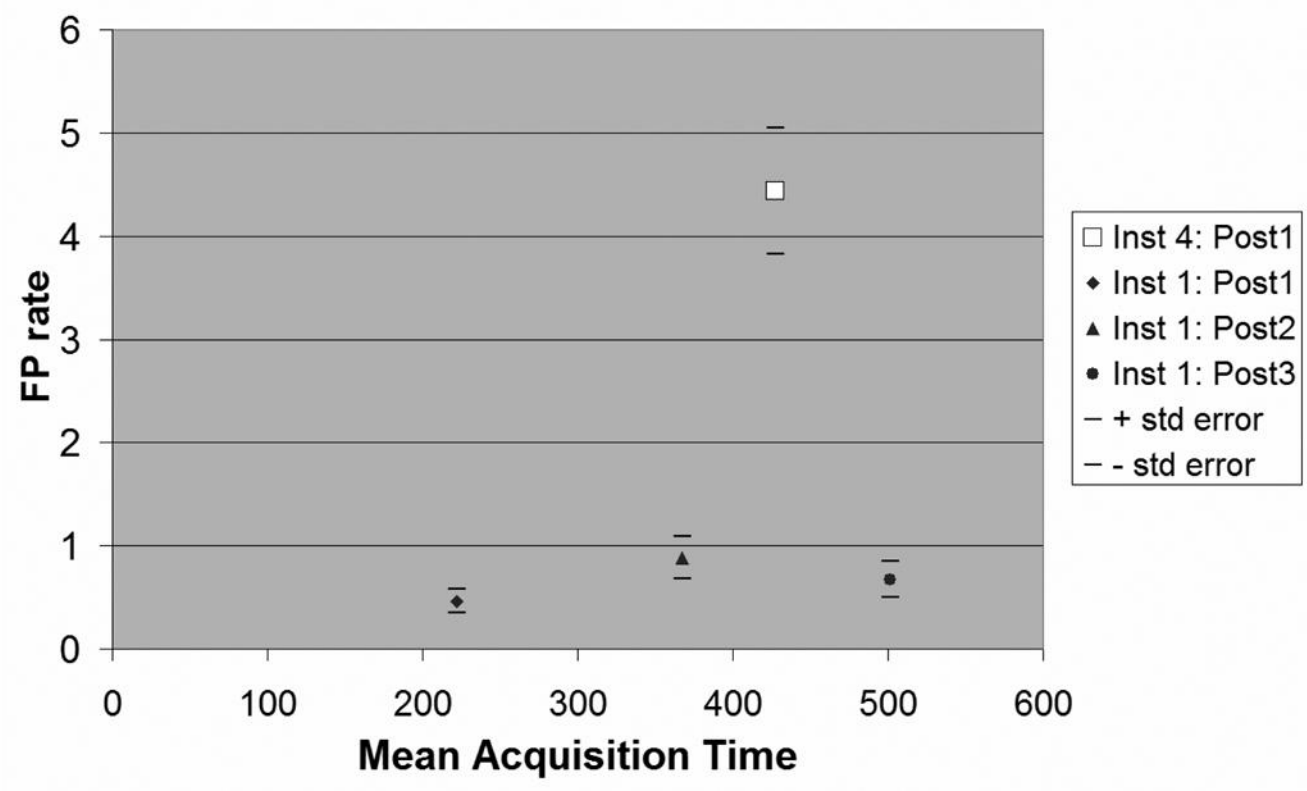

Fig 3.

False positive (FP) rates as a function of acquisition times. Solid markers show mean FP rates from Institution 1 for first 3 postcontrast series. Open square shows mean FP rate for Institution 4 for first postcontrast series. Horizontal lines show ± 1 standard error.

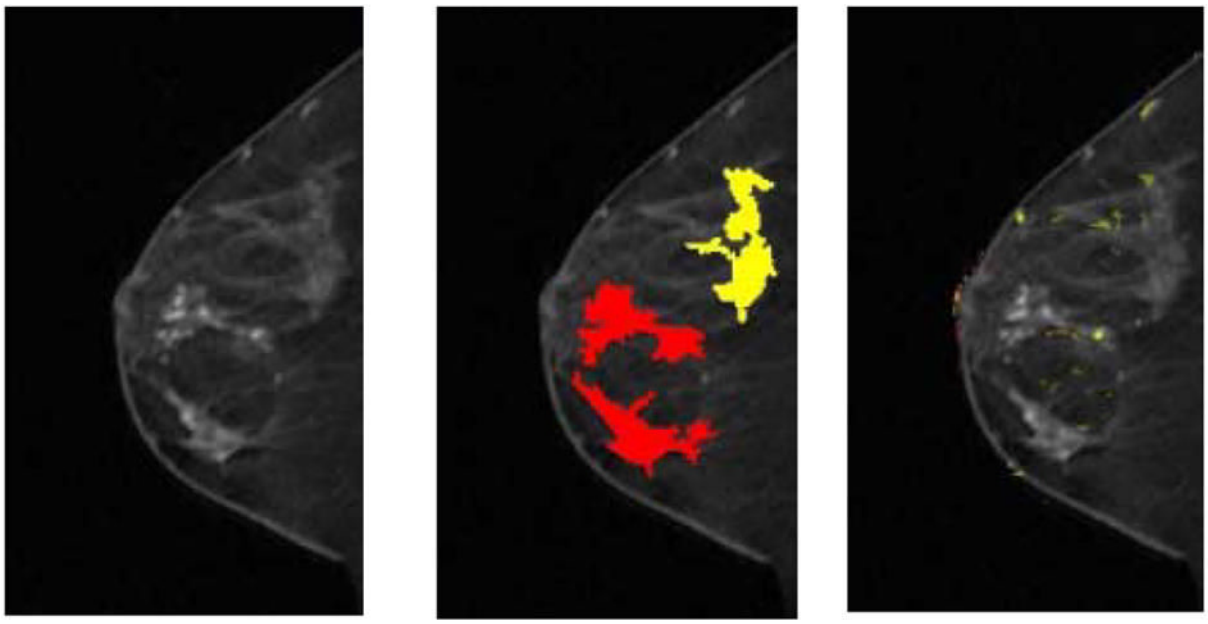

Fig 4. A 51-year-old female imaged on GE LX system. Patient had three areas identified on magnetic resonance as suspicious. All three were found to be infiltrating lobular carcinoma on final pathology. Only the subareolar mass was noted on mammography. Although all three regions with lobular carcinoma showed suspicious morphology, there are limited kinetic indications of malignancy

(a) First postcontrast T1 image, with a DICOM stamp showing a time of 202 seconds after precontrast image.

(b) Figure 4a overlaid with map showing positive morphologic blooming (red) and near-positive morphologic blooming (yellow).

(c) Figure 4a with a kinetic map overlay showing no significant areas of washout (red) plateau (yellow).

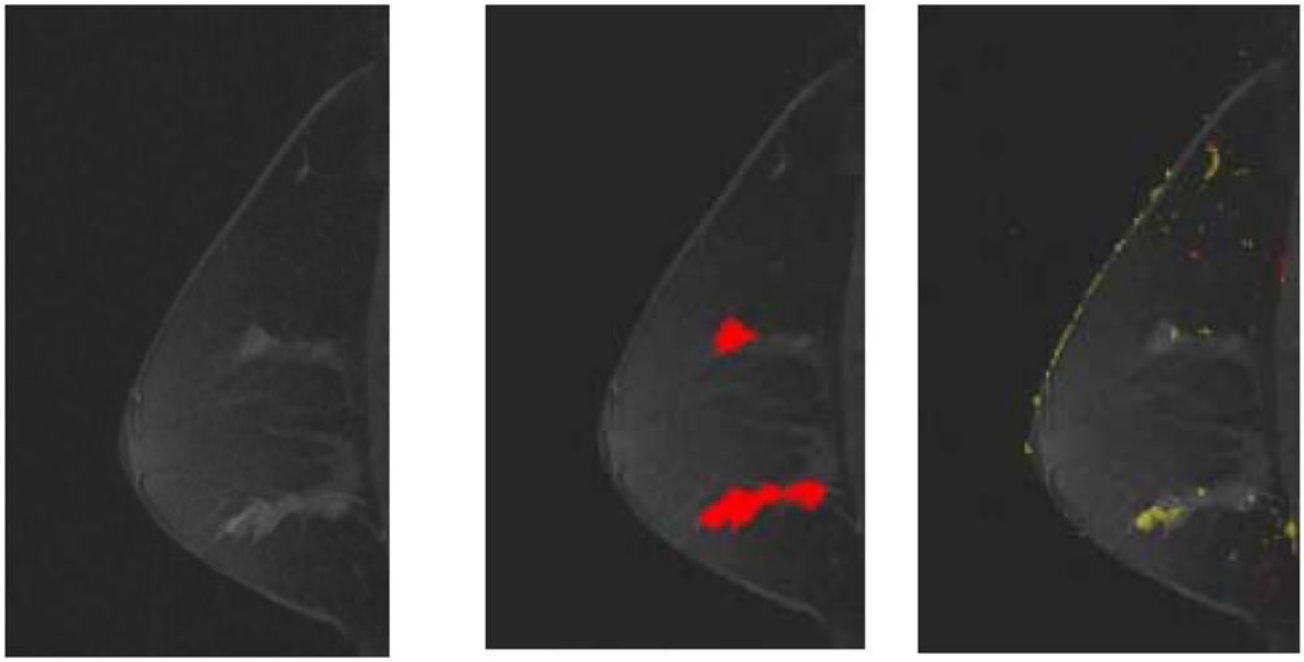

Fig 5. A 53-year-old female imaged on Siemens Magnetom system. Patient had two areas identified on magnetic resonance as suspicious. Both areas were found to be ductal carcinoma in situ Grades II-III on biopsy. The two regions identified as having suspicious morphologies match the regions with positive biopsies. Only the inferior lesion had suspicious kinetics

(a) First postcontrast T1 image, with a DICOM stamp showing a time of 904 seconds after precontrast image.

(b) Figure 5a overlaid with map showing suspicious morphologic blooming.

(c) Figure 5a with a kinetic map overlay showing no significant areas of washout (red) and a very small area of plateau (yellow) in anterior-inferior region.

Table 1

Systems and protocols used by institutions in multi-center study (Testing Data)

	Institution 1	Institution 2	Institution 3	Institution 4	Institution 5
MRI System	Siemens Sonata	Philips Intera	Siemens Magnetom	GE LX	GE Signa
Sequence	Spoiled gradient-echo	Gradient echo with Sense software	Gradient echo	FSPGR	FSPGR
Bilateral/Unilateral	Bilateral Interleaved	Unilateral	Unilateral	Unilateral and Bilateral Sequential	Bilateral affected breast first and bilateral contralateral breast first
Saline push after injection of gad?	Yes	No: 8 C/3 NC. Yes: 16C/1 NC	Yes	Yes	Yes
Matrix	256x256 and 512x512	179x256	256x256	256x292	256x256
cancerous (C) breasts	5	24	4	28	10
non-cancerous (NC) breasts	43	4	8	43	10
Basis of assessment of non-cancerous	No suspicious findings on MRI, ultrasound or mammo, no FU.	Biopsy of most suspicious lesion, No FU info available.	Mastectomy (3); Mammography with 6–14 mo. follow-up (5).	Imaging follow up min 6 mo. (29); no suspicious finding on MRI, no FU (14).	Biopsy of most suspicious lesion, No FU info available.
Data from DICOM headers: Minimum-Maximum (Mean)					
Interval between time of pre-contrast and time of post-contrast image used in study (sec)	115–317 (220)	157–534 (318)	241–904 (588)	170–784 (374)	373–1713 (943)
Echo time (msec)	1.8 – 6.5 (4.5)	5.9 – 6.5 (6.3)	4.5 – 4.5 (4.5)	2.3 – 5.0 (2.8)	1.8 – 2.4 (2.1)
Repetition time (msec)	7.7 – 26.0 (11.8)	32.9 – 33.0 (32.9)	11 – 20.0 (11.8)	17.0 – 20.0 (17.6)	17.0 – 24.6 (17.8)
Flip angle (deg)	25 – 30 (35.4)	55 – 55 (55.0)	35 – 40 (35.4)	35 – 45 (37.0)	35 – 35 (35.0)
Slice Thickness (mm)	2.2 – 4.2 (2.9)	3.0 – 4.4 (3.9) with 2 mm overlap	2.2 – 3.0 (2.9)	1.0 – 4.0 (3.0)	2.0 – 3.0 (2.9)
FOV (mm)	18 – 22 (20.0)	20 – 22 (20.2)	20 – 20 (20.0)	18 – 24 (20.3)	18 – 22 (19.6)

Table 2

FP rates in non-cancerous breasts for patients with/without cancer in contralateral breast

	Cancer absent in contralateral breast		Cancer present in contralateral breast	
	Number breasts	Mean FP/breast	Number breasts	Mean FP/breast
Institution 1	38	0.34	5	0.80
Institution 4	4	1.00	25	5.96
All 5 Institutions	42	0.48	38	4.29

Table 3

Definitions and statistics used in the analysis of Morphological Blooming and kinetics as complementary methods for detecting breast cancer

	Morphological Blooming	**Kinetics**	**Morphological Blooming plus Kinetics**
How evaluated	Computer analysis	Reader Interpretations	
Criteria for positive finding	Blooming value ≥10	Median finding of “plateau” or “washout”	Positive finding using either method
Sensitivity	78%	67%	89%
False negatives	10/45	15/45	5/45
Sensitivity on set of false negatives from complementary method	10/15 (67%)	5/10 (50%)	